

Effects of Persister Formation on Bacterial Response to Dosing

N. G. Cogan*

*Mathematics Department Tulane University New Orleans, LA. 70118 e-mail: cogan@math.tulane.edu
FAX: 504 865 5063

Abstract

Almost all moist surfaces are colonized by microbial biofilms. Biofilms are implicated in cross-contamination of food products, biofouling, medical implants and various human infections such as dental cavities, ulcerative colitis and chronic respiratory infections. Much of current research is focused on the recalcitrance of biofilms to typical antibiotic and antimicrobial treatments. Although the polymer component of biofilms impedes the penetration of antimicrobials through reaction-diffusion limitation, this does not explain the observed tolerance, it merely delays the action of the agent. Heterogeneities in growth-rate, also slow the eradication of the bacteria, since most antimicrobials are far less effective for non-growing, or slowly growing bacteria.

In this investigation, we describe the formation of 'persister' cells which neither grow nor die in the presence of antibiotics. We propose that the cells are of a different phenotype than typical bacterial cells and the expression of the phenotype is regulated by the growth rate and the antibiotic concentration. Based on several experiments which describe the dynamics of persister cells and which motivate a periodic dosing protocol, we introduce a mathematical model that describes the effect of such a dosing regiment. Results from simulations indicate that the relative dose/withdrawal times are important in determining the effectiveness of such a treatment. A reduced model is also introduced and the similar behavior is demonstrated analytically.

Keywords: Persister, tolerance, biofilm, model

1 Introduction

It has been estimated that 99% of all bacteria live in structured communities termed biofilms [3]. Recently the US National Institutes of Health announced that, "Biofilms are medically important, accounting for over 80% of microbial infections in the body". These two observations, in conjunction with the observation from numerous sources [12, 13, 31, 2, 19, 29] that typical antimicrobial treatments fail to eradicate the bacteria, leads one to the conclusion that understanding resistance mechanisms for bacterial biofilms is of paramount importance in treating bacterial infections. There are several hypotheses concerning resistance mechanisms which can be placed into three broad categories: transport limitation, physiological tolerance and phenotypic resistance.

There are several well documented examples of how the biofilm structure can prevent an applied antimicrobial agent from reaching the entire bacterial population by mechanisms such as a neutralizing reaction with components of the biofilm [50, 15], synthesis of an antimicrobial degrading enzyme [21, 4] and adsorption of the antimicrobial by the exo-polymeric substance (EPS) [28]. There are been several mathematical models of biofilm disinfection which address this mechanism by including reduced diffusion and various antimicrobial-degrading reactions [41, 17, 9]. These studies have indicated that if the reaction is catalytic and does not degrade the neutralizing agent, bacteria deep within the biofilm are not exposed to the antimicrobial agent. Otherwise, even though lowered diffusion and degrading reactions slow the penetration, the antimicrobial will eventually penetrate the entire biofilm exposing the entire population of bacteria to the agent. Unless there are other mechanisms at work which protect bacteria from the agent, all bacteria would be killed.

Because most biocides and antibiotics are more effective at killing respiring bacteria [12], the effectiveness of typical antimicrobials will be spatially dependent. In particular, there will be regions within the biofilm where the bacteria are drastically less susceptible to disinfection. This protective mechanism is termed physiological resistance. Mathematical models addressing this issue [9, 39] indicate that bacteria on the surface of the biofilm are killed before those deep within the biofilm; however, this mechanism cannot act alone, since the nutrient penetrates further as the bacteria are killed. Models of this mechanism indicate that constant exposure to antimicrobials will eventually result in complete eradication of the bacteria.

The focus of this paper is on the last resistance mechanism: phenotypic resistance. Because both mechanisms described above cannot explain the typical bi-phasic nature of survival data, tolerance due to phenotypic variation is currently being studied [45, 31]. It has been shown that quorum sensing mechanisms, known to be linked with biofilm formation [14], may also be linked to antibiotic resistance [33, 18, 45]. Quorum sensing is involved in up-regulation of multi-drug efflux pumps [5], although this may not play a role in the antibiotic-resistant phenotype [26]. Another study by Sufya [45], indicates that variations in the maximum specific growth rates can result in variations in the susceptibility of bacteria. A novel explanation is the existence of 'persister' cells which are extremely tolerant of antibiotics. The physiology of such cells is not currently well understood, although their existence has been demonstrated [16, 25, 31]. As yet there is no consensus as to what phenotypic variations are primarily responsible for biofilm tolerance [31].

The goal of the current investigation is to incorporate current biological observations into a mathematical model of bacterial tolerance with the aim of proposing new dosing strategies and experimentally verifiable hypotheses. Although the model applies to homogeneous populations of bacteria, understanding the kinetics of the bacteria is the first step towards a more realistic model in a biofilm setting. We first summarize the experiments that motivate the model. We then describe our assumptions and the consequent model. Several simulations aimed at estimating parameters, exploring dosing protocols and exposing fundamental issues will be described. Finally, we introduce a simplified model which can be treated analytically.

2 Planktonic Experiments

Bacterial tolerance to antibiotics has been well established although the specific mechanisms are still being investigated. In two papers [16, 25], the susceptibility of different species of bacteria at different stages of growth is investigated. In the first of these, Desai [16] explores the tolerance of both planktonic and biofilm cultures of *B. cepacia* bacteria to ciprofloxacin and ceftazidime. Bacterial populations were grown in rotary shakers (planktonic) and polycarbonate membranes (biofilm). At given times, samples of comparable bacterial number were taken, diluted and exposed to the antibiotics for one hour. After the exposure, resistance data was shown by plotting the ratio of the exposed population to the untreated population on a logarithmic scale. By sampling at different times, resistance is linked to the growth stage. That is, the untreated population showed logistic growth with little or no lag stage, followed by exponential growth and then a drop in the growth rate due to nutrient limitation. Both planktonic and biofilm bacteria showed drastic increase in tolerance to both

antibiotics during during exponential growth. Thus, the growth rate/phase of the culture plays an important role in determining antibiotic susceptibility. In this study the planktonic bacteria are always more susceptible to biofilm bacteria at equivalent stages of growth although this result has been contradicted [42]. Because the biofilm cultures were disrupted and suspended before treating them, the increased resistance is not from any physical barrier. Rather, tolerance results from physiological and phenotypic variations.

The second paper describes similar experiments on planktonic populations of *E. coli*, *P. aeruginosa* and *S. aureus*. Here, cultures of bacteria were cultured in a shaker overnight. At designated times 1 ml of cells were treated with antibiotics for three hours and surviving bacteria were enumerated. The focus of this investigation is on the generation of persisters, cells which neither grow nor die in the presence of antibiotics. The investigators first determine the time-dependent killing of bacteria in the exponential phase, by incubating a culture for three hours and then exposing the cells to antibiotics. The population is enumerated at specified times. To measure the effect of the antibiotic, the ratio between the surviving population and the initial population is plotted on a logarithmic scale. The survival curves show that within 0.5-1 hour, more than 99% of the cells are killed. After that, there is almost no change in the surviving population indicating the existence of ‘persister cells’.

The investigators then show that the persisters cells are not mutants by re-suspending the bacteria and culturing them with aeration for 16-24 hours and demonstrating that the survival curves are the same for all four replicates. Next the growth-state dependence of persisters is determined by challenging samples of a growing culture at designated times for three hours. The results indicate that the level of persister formation was constant during the lag and early exponential phases. During the mid-exponential phase the number of persisters increased. Persisters can be eliminated by diluting the persisters from the mid-exponential phase in fresh medium and re-exposing them to antibiotics. These results were qualitatively similar across all species tested.

In both studies is that antibiotics with different targets are used, a β -lactam and a fluoroquinolone. This is important, because fluoroquinolones are known to be effective against non-growing cells, indicating a more complicated resistance mechanism than physiological resistance.

In the following sections we describe our mathematical model. The model consists of three ordinary differential equations (ODE) which govern the dynamics of the susceptible and persistent bacteria and one growth limiting substrate. In the absence of antibiotic, the susceptible bacteria consume substrate and reproduce. When antibiotic is added, a fraction of the the susceptible cells are killed while another fraction convert to persister cells. Persister cells are not effected by the antibiotic, nor do they grow. Instead, if there is no antibiotic, persister cells revert to susceptible cells at a fixed rate.

3 Model Assumptions and Description

We denote the two phenotypes as B_s and B_p for susceptible and persister density, respectively. We assume that there is one growth-limiting substrate, S and one antibiotic, denoted A . The population of susceptible bacteria changes due to growth, death due to antibiotic action, loss due to transition to persister cells and gain as the persistent cells revert back to susceptible

cells. Thus, the equation governing the dynamics of the susceptible population is given qualitatively as,

$$\frac{dB_s}{dt} = \underbrace{g(B_s, S)}_{\text{Growth}} - \underbrace{d(B_s, S, A)}_{\text{Disinfection}} - \underbrace{l(B_s, S, A)}_{\text{Loss}} + \underbrace{r(B_p, S, A)}_{\text{Reversion}}. \quad (1)$$

We assume that the growth is described by Monod kinetics with maximum specific growth rate, Monod coefficient and yield denoted μ_{max} and K_s and Y , respectively. Thus the growth term is

$$g(B_s, S) = \frac{\mu_{max}}{Y} \frac{S}{K_s + S} B_s.$$

Disinfection of the susceptible population depends on the type of antibiotic used. If the antibiotic is a beta-lactam then the disinfection rate is assumed to be proportional to the growth rate. If the antibiotic is a fluoroquinolone we allow for disinfection in the absence of growth, although at a reduced rate. We assume that the disinfection term in Equation (1) is

$$d(B_s, S, A) = k_d(A, t) \mu_{max} \frac{S + \alpha}{K_s + S} B_s,$$

where α is zero for beta-lactam and non-zero for fluoroquinolone. The function $k_d(A, t)$ depends on the antibiotic concentration. In particular, $k_d = 0$ if $A = 0$ and is nonzero otherwise. Because we are interested in dosing strategies which are time dependent the disinfection rate is necessarily time dependent.

The loss of susceptible cells to the persister population is assumed to occur at a rate proportional to the growth rate and depends on the antibiotic concentration. Thus

$$l(B_s, S, A) = k_l(A, t) \mu_{max} \frac{S}{K_s + S} B_s. \quad (2)$$

Again, the transition from susceptible to persister is assumed to be caused by exposure to the antibiotic so this rate is also time dependent.

Persister cells can revert to susceptible cells as long as the applied antibiotic concentration is zero. Otherwise, there is no reversion back to susceptible cell type. Mathematically we have $r(B_p, S, A) = k_g(A, t) B_p$, where k_g is zero if there is antibiotic present and non-zero otherwise.

Putting these together gives the equation governing the dynamics of the susceptible population as

$$\frac{dB_s}{dt} = \frac{\mu_{max}}{Y} \frac{S}{K_s + S} B_s - k_d(A, t) \mu_{max} \frac{S + \alpha}{K_s + S} B_s - k_l(A, t) \mu_{max} \frac{S}{K_s + S} B_s + k_g(A, t) B_p. \quad (3)$$

The persister cells are not killed by the antibiotic. The population changes by conversion to and from susceptible cells. The governing equation is,

$$\frac{dB_p}{dt} = k_l(A, t)\mu_{max}\frac{S}{K_s + S}B_s - k_g(A, t)B_p. \quad (4)$$

Here we have assumed that the persister population does not grow; either growth is being inhibited by the antibiotic or persister cells revert to susceptible cells.

The substrate is being consumed by the susceptible population,

$$\frac{dS}{dt} = -\mu_{max}\frac{S}{K_s + S}B_s. \quad (5)$$

Equations (3) - (5) describe the dynamics for suspended populations of susceptible and persisting bacteria and substrate. In the next section, we describe simulations which yield results comparable to experimental results shown in [25] and [16]. Then we show results from a simulated dosing protocol entailing application of a constant concentration of antibiotic for a specified length of time, withdrawing the antibiotic and allowing the population to regrow. We see that results depend dramatically on the length of dose/withdrawal times. In particular, we will show that for short withdrawal times, we generate a persister population which is eliminated extremely slowly. If the treatment is terminated before the persister population is cleared, there is rapid regrowth of the bacterial population. If the withdrawal time is very long, the susceptible population is only transiently eliminated. The persister cells, generated from the dosing step are a source for the susceptible population, which will regrow given enough time. There is a dosing regiment for which neither of these cases occurs; instead, both bacterial populations are eliminated.

Following this section, we introduce a simplified model which is amenable to analytic treatment, but still retains the fundamental behavior of successful treatment for intermediate dose/withdrawal times.

3.1 Parameters

There are several parameters that are of interest, values used in the simulations are shown in Table I. We have used typical values for maximum growth rate, yield and Monod coefficient. The four parameters which depend on the antimicrobial agent, k_d , α , k_l and k_g were estimated. We assume that the rates are linearly proportional to A . The parameters regarding disinfection rate were chosen to fit the time-dependent kill curve in [25]. The rate of transformation from susceptible to persister cells was estimated from the data in [25]. We assume that the persister cell lose their persister phenotype on a time scale longer than that of growth.

Results from fitting the time-dependent killing from [25] are shown in Figure (1). We are primarily concerned with matching the bi-phasic nature and time-scale for the plateau region and also the effectiveness of each antibiotic. Comparing the predicted survival curves with the data indicate that our model is capturing both the gross qualitative trends as well as the correct scales.

Once the parameters have been fixed, we simulate the growth-stage dependence of persister formation. In the experiments, bacteria were disinfected as a suspension. Periodic

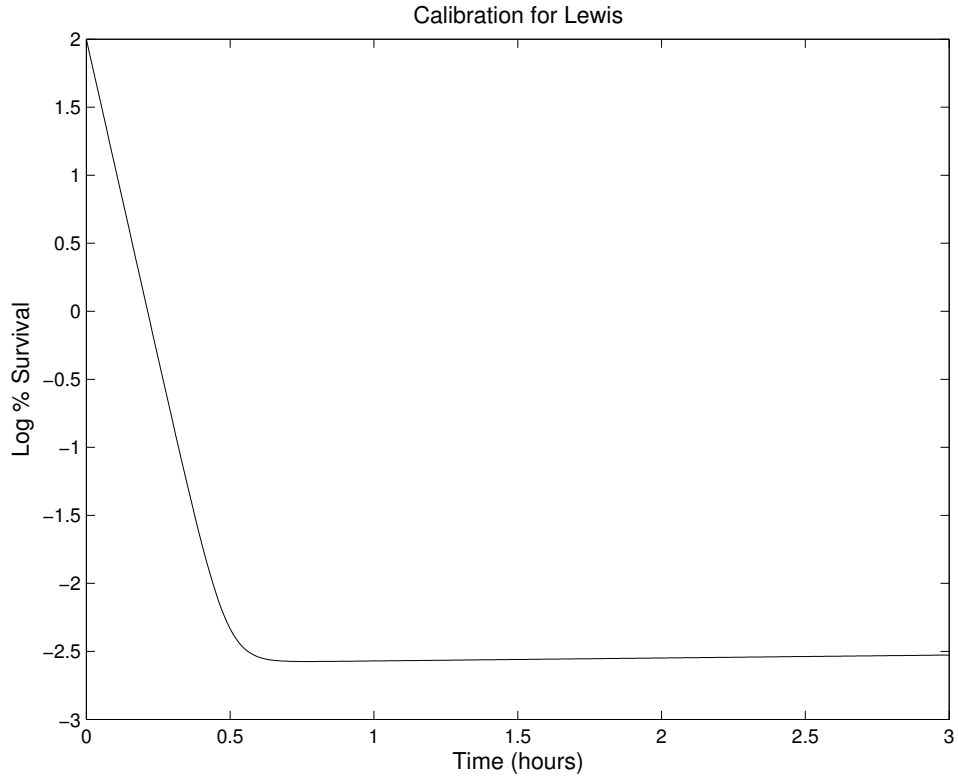


Figure 1: Time-dependent killing curve for cells treated with antibiotic. This qualitatively agrees with data from [25] and shows the distinct bi-phasic nature, typical for antibiotic treatment. We are primarily concerned with the time scale associated with clearance and our parameters have been chosen so that the plateau region begins within the first $\frac{1}{2}$ hour. The parameters are listed in Table I.

Parameter	Symbol	Units	Value	Source
Maximum Specific Growth Rate	μ_s	h^{-1}	0.417	[39]
Yield Coefficient	Y		0.2	[39]
Monod Coefficient	K_s	mg l^{-1}	0.2	[39]
Maximum Disinfection Rate	k_d	h^{-1}	40	Estimated
Non-growing Disinfection	α	mg l^{-1}	0.07	Estimated
Rate of Loss	k_l	h^{-1}	0.001	Estimated
Rate of Gain	k_g	h^{-1}	0.05	Estimated

Table I: Parameters used in the simulations.

samples were taken from the reactor and exposed to antibiotic and then enumerated. This generates two curves, an untreated growth curve and a treated growth curve. We began with initial conditions corresponding to 1×10^7 susceptible cells, zero persister cells and substrate concentration of twice K_s . The time-dependent behavior of the bacteria and substrate are determined by solving Equations (3) - (5) using the package ODE45 in MATLAB. Once the untreated simulation is completed, we use values of B_s , B_p and S at specified times, and simulate the effect of exposure to antibiotic for either one or three hours, corresponding to the experiments in [16] and [25], respectively. In [25] data for the cell counts for treated and untreated are shown on a logarithmic scale. In [16] the data is given as ratio of the number of surviving cells to the initial cell count, on a logarithmic scale, our results are shown on comparable axis in Figures (2)- (5).

3.2 Simulated Dosing Experiment - ODE

In this section we describe results from a simulated dosing experiment. In [31], Lewis describes a possible treatment to eradicate all persisters. The treatment requires applying an antibiotic for a period of time, killing all susceptible bacteria while generating small population of persister cells. Withdrawing the antibiotic allows the persister cells to grow. As the persisters grow they lose the persister phenotype, reverting back to susceptible cells. At this point a second application will remove virtually all of the bacteria.

In this section, we describe simulations to test this hypothesis. We begin our simulations with a population of susceptible cells. The cells are exposed to nutrient, initially twice the half-saturation value, and an antibiotic for a fixed length of time, termed dose period and denoted T_d . This kills the susceptible cells quickly and generates a small population of persister cells. We then remove the antibiotic and allow the cells to grow for a fixed length of time, termed withdrawal period and denoted T_w . Persister cells revert to susceptible cells, which then consume nutrient and grow. This completes one dose/withdrawal period. After one dose/withdrawal period, fresh nutrient is added and the cycle is repeated. Results from the experiment, with a dose period of 10 hours and varying withdrawal period are shown in Figures (6)- (9). If the bacterial population is not eliminated within approximately 30 days, the treatment is deemed ineffective and the simulation is stopped.

Here we see a very interesting result. For very short withdrawal periods, the treatment

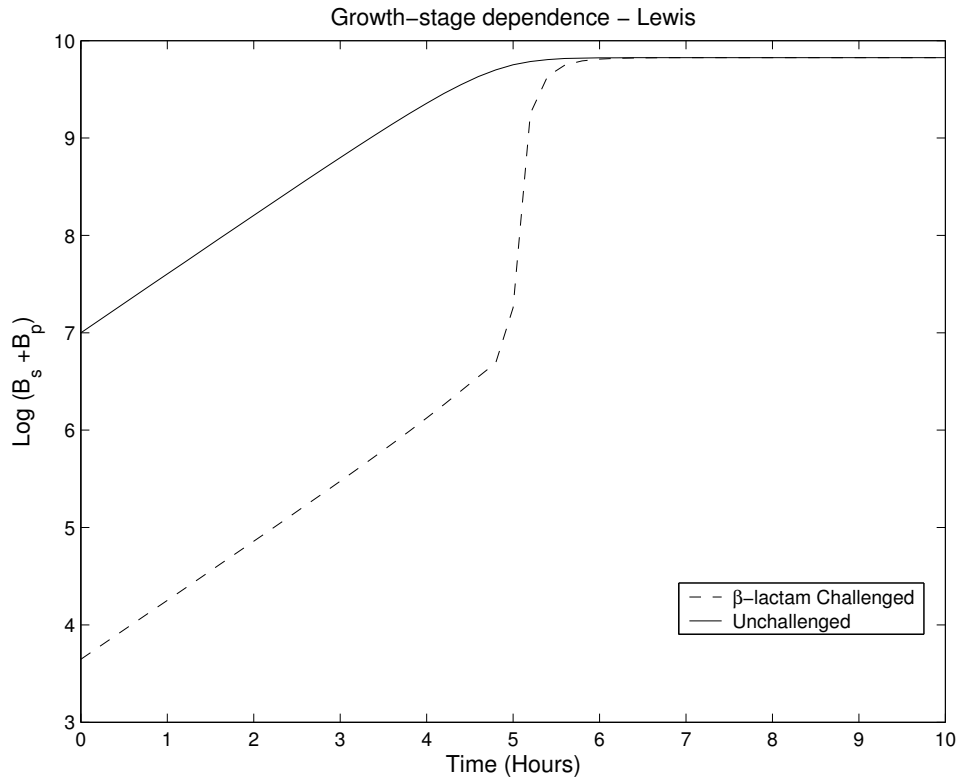


Figure 2: Growth-stage dependence of persister formation for bacteria challenged with a β -lactam (growth-rate dependent) antibiotic. We see an abrupt increase in the number of surviving bacteria at approximately five hours. Our results agree well with the data in [25]. We also see that as the growth-rate goes to zero because of nutrient depletion the entire population becomes tolerant.

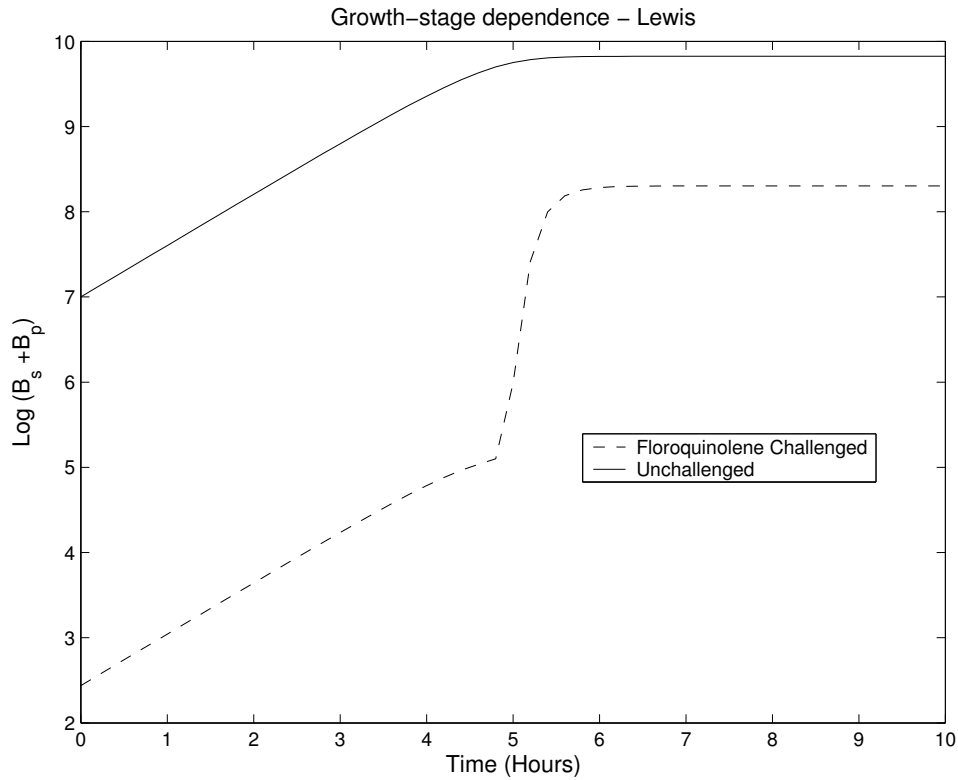


Figure 3: Growth-stage dependence of persister formation for bacteria challenged with a fluoroquinolone (non-growth-rate dependent) antibiotic. We see an abrupt increase in the number of surviving bacteria at approximately five hours. Our results agree well with the data in [25]. Because the antibiotic is effective against non-growing cells, we do not see saturation to the untreated cell count as in Figure (2). Instead, the cell count saturates to a lower level.

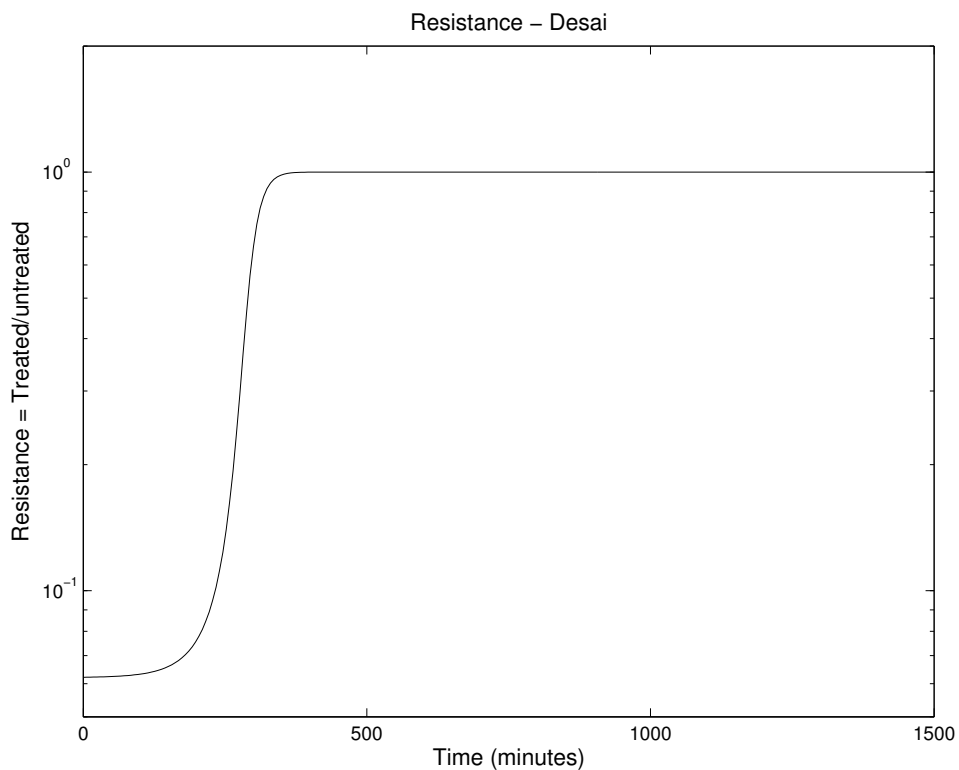


Figure 4: Growth-stage dependence of persister formation for bacteria challenged with a β -lactam (growth-rate dependent) antibiotic. Our results are plotted on a scale defined in [16] for comparison. We see an abrupt increase in the number of surviving bacteria at approximately 250 minutes which increases until the nutrient is depleted and the entire population becomes tolerant.

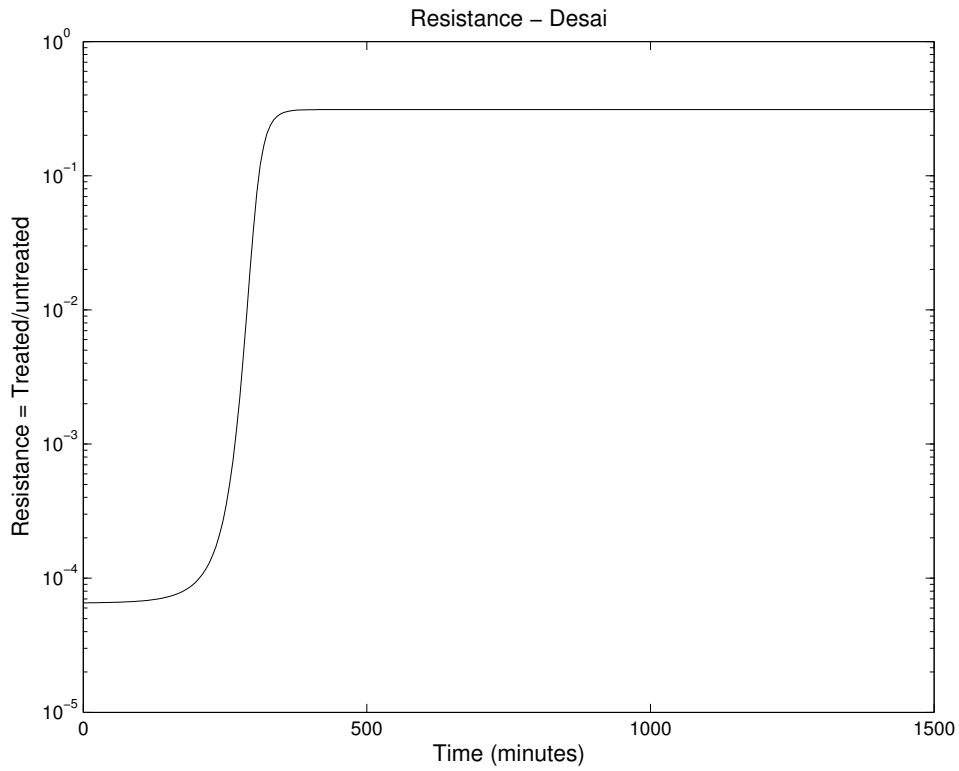


Figure 5: Growth-stage dependence of persister formation for bacteria challenged with a fluoroquinolone (non-growth-rate dependent) antibiotic. Because the antibiotic is effective against non-growing cells, we do not see saturation to the untreated cell count as in Figure (4). Instead, the cell count saturates to a lower level.

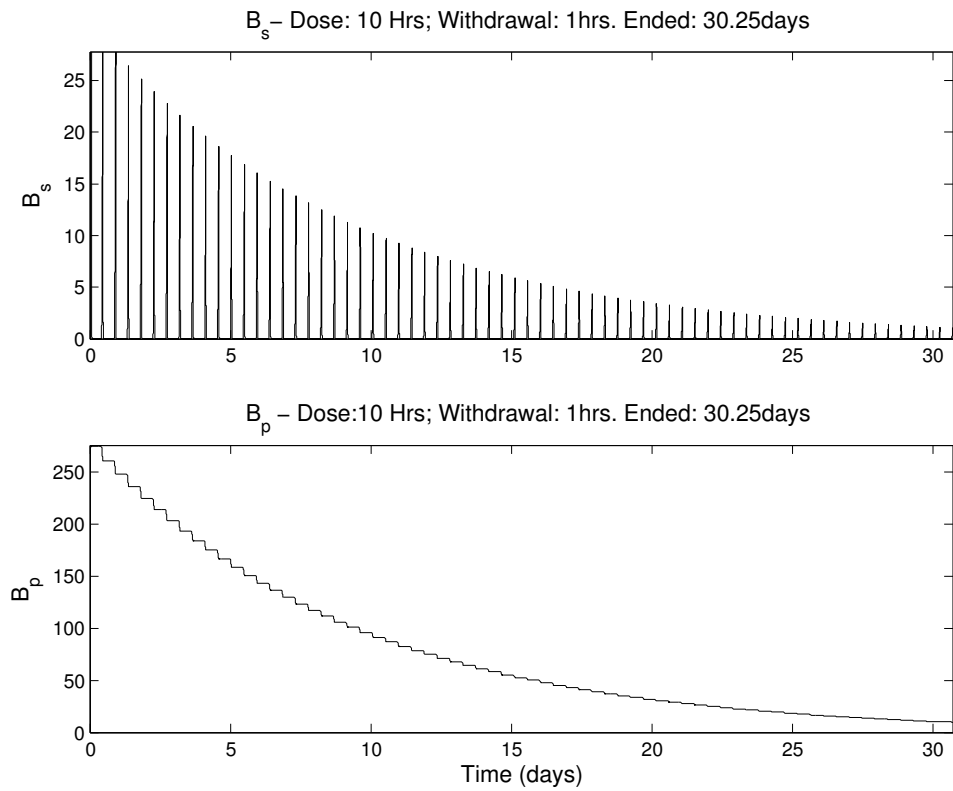


Figure 6: Periodic dosing experiment with withdrawal period of one hour. We see that, while the susceptible cells are killed, the persister population is being killed very slowly. This treatment was not successful.

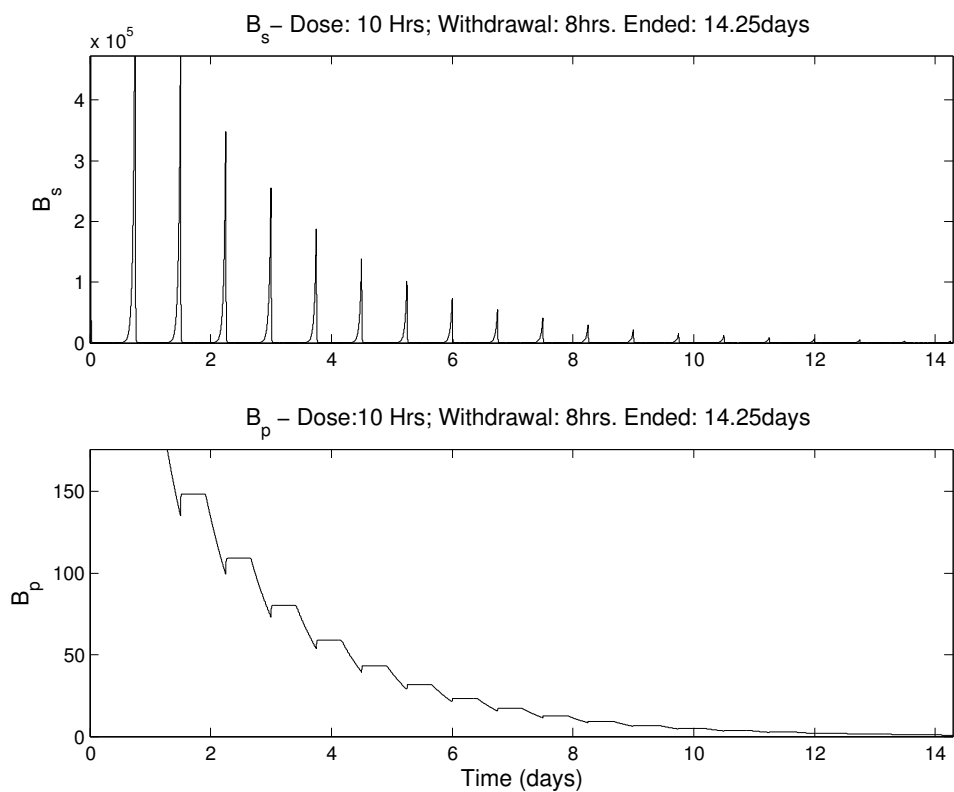


Figure 7: Periodic dosing experiment with withdrawal period of eight hours. We see that both the susceptible and persister cells are killed indicating a successful treatment.

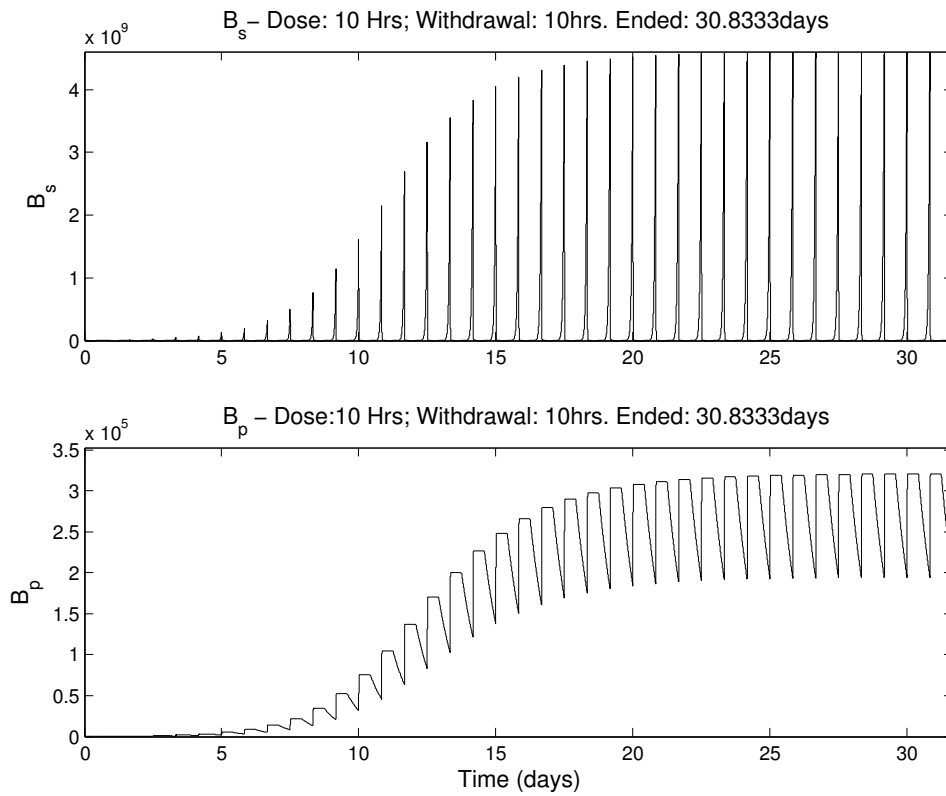


Figure 8: Periodic dosing experiment with withdrawal period of ten hours. We see that neither the susceptible nor the persister cells are eliminated. This treatment was not successful.

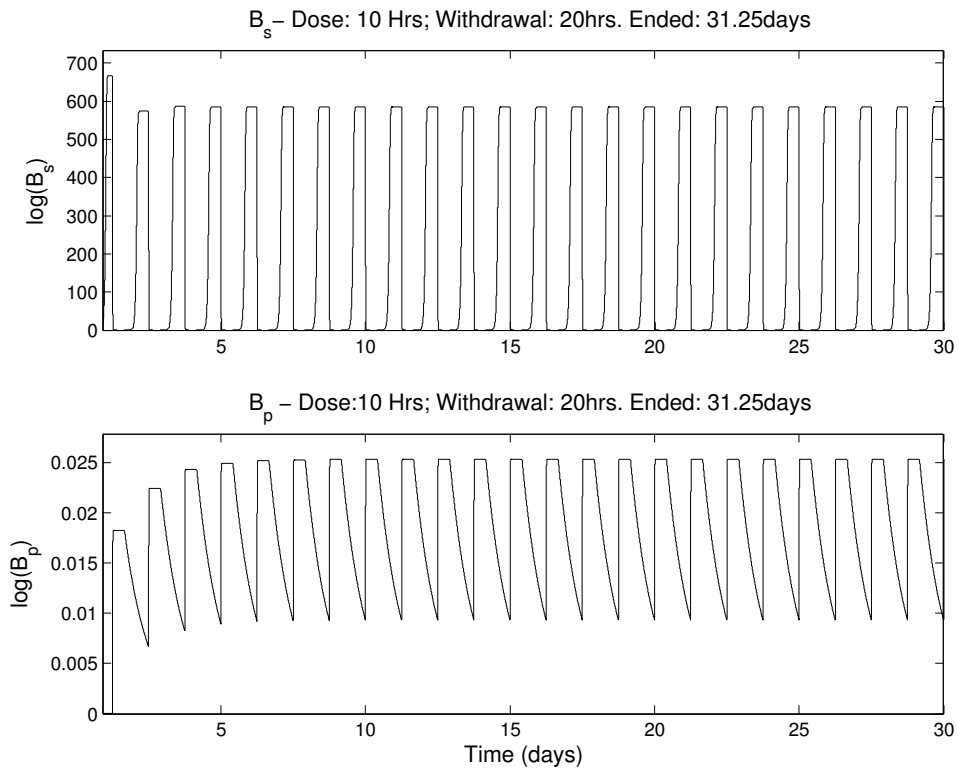


Figure 9: Periodic dosing experiment with withdrawal period of twenty hours. We see that neither the susceptible nor the persister cells are eliminated. This treatment was not successful.

fails to eliminate the persister population within the allotted time period (see Figure (6)). If the treatment is discontinued, the population will quickly regrow. For extremely large withdrawal periods, the susceptible population is not eliminated. Instead, it responds to the treatment quickly, but the persister population is a source of susceptible cells, which regrow to the carrying capacity before the next dose period. Again this results in an ineffective treatment (see Figures (8) and (9)). However, there is an intermediate dose/withdrawal pair, for which the treatment is effective in clearing both the susceptible and persister population. This indicates that periodic dosing may be effective, but the dosing regiment must be specific to the bacterial kinetics. Specifically, the withdrawal period must be long enough to allow the persister cells to revert to susceptible cells, but not long enough for the susceptible cells to reach the exponential growth stage.

The effectiveness of the dosing strategy depends on the number of susceptible and persister cells that are not killed. Clearly this depends on the dosing strategy. To find the optimal withdrawal length, we measure the change in the population as a function of the this length. We first define the envelope of the survival curves as the maximum, during each cycle, of the respective populations. An example of the survival curve and the envelope is given in Figure (10). The slope of the envelope on a logarithmic scale gives the exponential rate of decrease or increase of the population. For successful treatments (i.e. those for which the each of the populations tends to zero), the maximum rate is negative. In Figure (11), we show the maximum slope of the logarithm of the envelope as a function of the withdrawal time. Minimizing this curve gives the optimal strategy which for the parameters given in Table I and $Td = 10$ hours, is to withdraw the antibiotic for approximately 7.5 hours.

Results from the simulations predict that there is an optimal dosing strategy. However, because the differential equations are nonlinear and non-autonomous it is difficult to proceed with any analytic treatment. In the following section, we propose a simplified model by assuming that the nutrient level is constant. This reduces the model from a system of three coupled nonlinear, non-autonomous equations to a system of two linear, non-autonomous equations. These equations can be solved analytically and the dynamics of the populations of susceptible and persistent bacteria reduce to a two-dimensional map. Therefore the growth/decay of the populations can be determined by the eigenvalues of the map, which depend on the parameters of the model.

4 Simplified Model

We assume that the nutrient is maintained at a constant level, hence S is constant. The model reduces to

$$\frac{dB_s}{dt} = \hat{k}_s B_s - \hat{k}_d(A, t) B_s \tag{6}$$

$$- \hat{k}_l(A, t) B_s + \hat{k}_g(A, t) B_p$$

$$\frac{dB_p}{dt} = \hat{k}_l(A, t) B_s - \hat{k}_g(A, t) B_p. \tag{7}$$

We further assume that the antibiotic level switches instantaneously from application to withdrawal. Under these assumptions, \hat{k}_s is a positive constant while \hat{k}_d and \hat{k}_l are zero

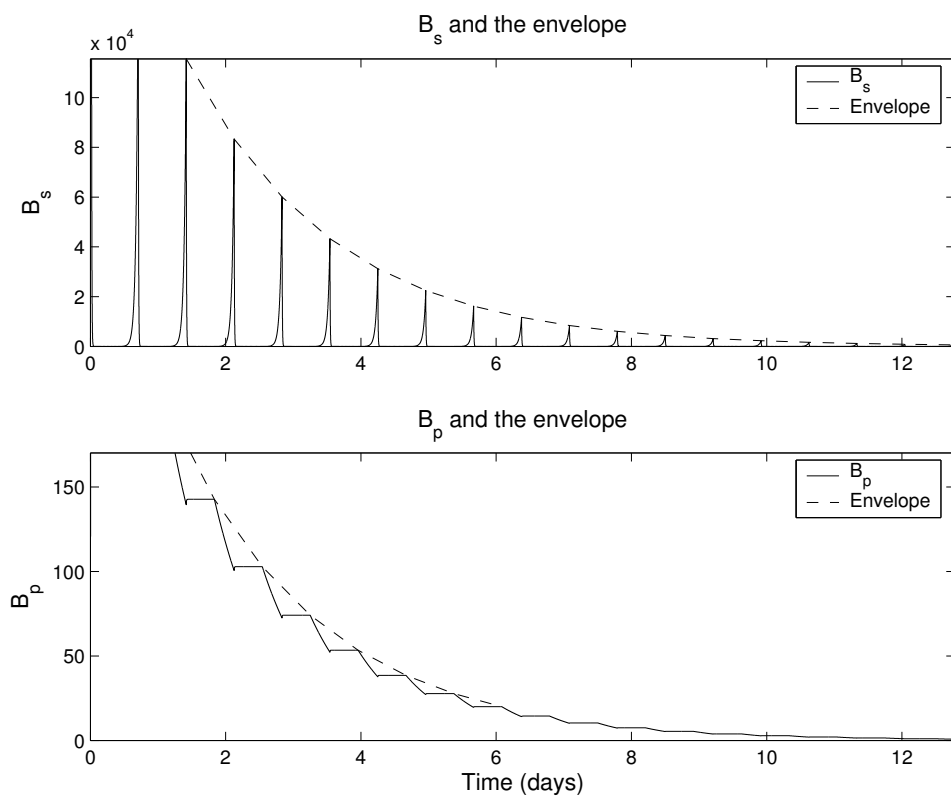


Figure 10: Survival curves for susceptible and persister cells along with the envelopes of the curves. The envelopes are given by the maximum of the populations during the dosing cycle. This gives an overall view of the effect of the dosing strategy.

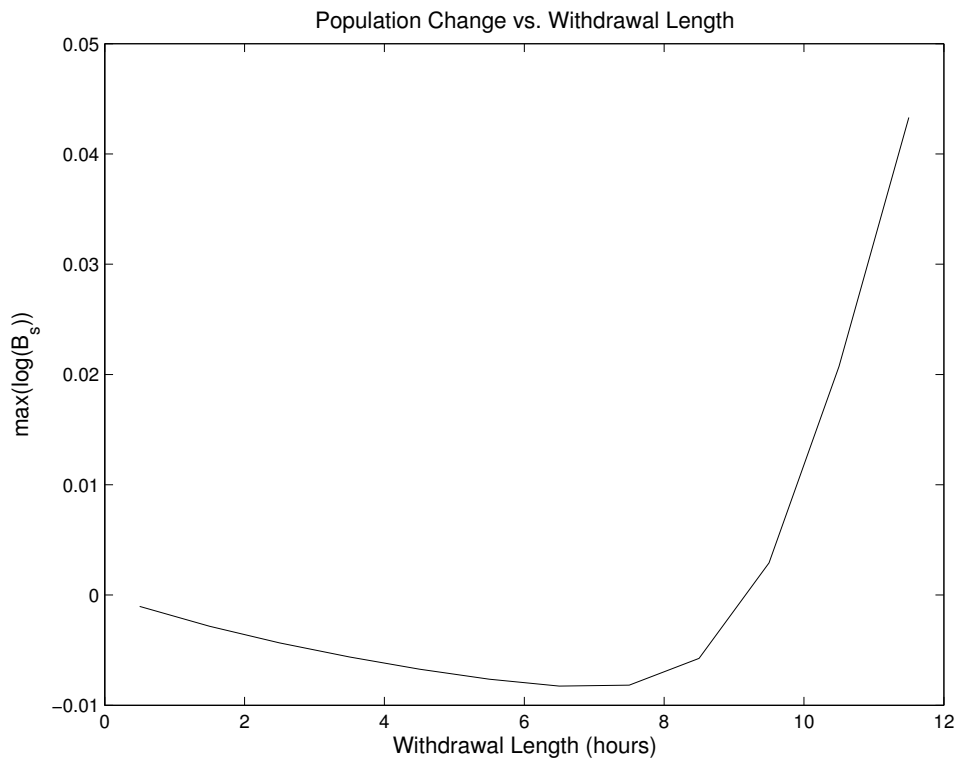


Figure 11: Maximum rate of change for the population of cells as a function of the withdrawal length. The maximum rate of change of envelope of the population is calculated for various withdrawal lengths. We see that for withdrawal time shorter than approximately 9 hours, the treatment is effective. For withdrawal periods longer than this, the overall population actually increases. The minimum of this curve gives the optimal withdrawal time of approximately 7.5 hours for the parameters used.

if there is no antibiotic and non-zero otherwise. The rate of reversion from persister to susceptible described by \hat{k}_g is non-zero only if the antibiotic is not applied. With these assumptions, the dynamics for the populations during each phase (i.e. dose or withdrawal) are easily calculated. The solution to Equations (6) and (7) with initial conditions $B_s(0)$ and $B_p(0)$ are

$$B_s(t) = \begin{cases} B_s(0)e^{(\hat{k}_r - \hat{k}_d - \hat{k}_l)t} & A \geq 0 \\ \frac{(B_s(0) + B_p(0))\hat{k}_g + B_s(0)\hat{k}_r}{\hat{k}_g + \hat{k}_r} e^{\hat{k}_r t} - \frac{B_p(0)\hat{k}_g}{\hat{k}_g + \hat{k}_r} e^{-\hat{k}_g t} & A = 0, \end{cases}$$

and

$$B_p(t) = \begin{cases} B_p(0) + \hat{k}_l B_s(0) \frac{e^{(\hat{k}_r - \hat{k}_d - \hat{k}_l)t} - 1}{\hat{k}_r - \hat{k}_d - \hat{k}_l} & A \geq 0 \\ B_p(0)e^{-\hat{k}_g t} & A = 0. \end{cases} \quad (8)$$

The dynamics of a population of susceptible and persistent bacteria, with constant nutrient and periodic antibiotic application and withdrawal is fully described by the above equations. If we begin with an initial population of bacteria which are all susceptible (i.e. $(B_s(0) = B_s, B_p(0) = 0)$) and apply an antibiotic for a length of time T_d , the population of each phenotype is

$$B_s(T_d) = B_s(0)e^{(\hat{k}_r - \hat{k}_d - \hat{k}_l)T_d} \quad (9)$$

$$B_p(T_d) = \hat{k}_l B_s(0) \frac{e^{(\hat{k}_r - \hat{k}_d - \hat{k}_l)T_d} - 1}{\hat{k}_r - \hat{k}_d - \hat{k}_l}. \quad (10)$$

Using these values as initial conditions for the dynamics with $A = 0$ for a length of time T_w , we obtain the new populations

$$B_s(T_w) = \frac{(B_s(T_d) + B_p(T_d))\hat{k}_g + B_s(T_d)\hat{k}_r}{\hat{k}_g + \hat{k}_r} e^{\hat{k}_r T_w} - \frac{B_p(T_d)\hat{k}_g}{\hat{k}_g + \hat{k}_r} e^{-\hat{k}_g T_w} \quad (11)$$

$$B_p(T_w) = B_p(T_d)e^{-\hat{k}_g T_w}. \quad (12)$$

We define M as the map taking $(B_s(0), B_p(0))$ to $(B_s(T_w), B_p(T_w))$. This map can be written as a matrix with entries

$$M_{1,1} = \frac{(\hat{k}_r^2 + \hat{k}_g \hat{k}_r - \hat{k}_r \hat{k}_d - \hat{k}_g \hat{k}_l - \hat{k}_g \hat{k}_d) e^{\hat{k}_r T_w + (\hat{k}_r - \hat{k}_d - \hat{k}_l) T_d} - \hat{k}_g \hat{k}_l e^{-\hat{k}_g T_w}}{(\hat{k}_g + \hat{k}_r)(\hat{k}_r - \hat{k}_d - \hat{k}_l)} \quad (13)$$

$$M_{1,2} = \frac{\hat{k}_g}{\hat{k}_g + \hat{k}_r} (e^{\hat{k}_r T_w} - e^{-\hat{k}_g T_w}) \quad (14)$$

$$M_{2,1} = \frac{\hat{k}_l}{\hat{k}_r - \hat{k}_d - \hat{k}_l} (e^{(\hat{k}_r - \hat{k}_d - \hat{k}_l) T_d} - 1) e^{-\hat{k}_g T_w} \quad (15)$$

$$M_{2,2} = e^{-\hat{k}_g T_w}. \quad (16)$$

The success or failure of the dosing strategy in this simplified situation is determined by the eigenvalues of the map M . If the magnitude of each eigenvalues is less than one, the

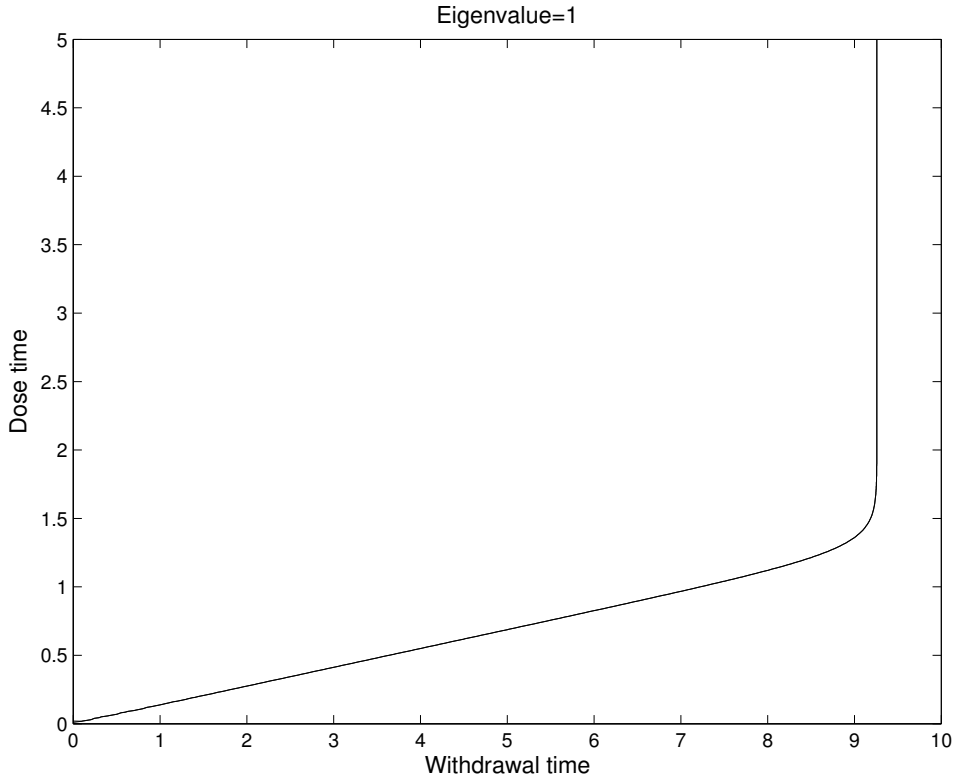


Figure 12: We show the curve in the Td, Tw -plane for which the eigenvalue is equal to one. Above this curve, the eigenvalue is less than one, while below this curve the eigenvalue is greater than one.

repeated dose/withdrawal will eventually eradicate both populations. Otherwise there will be growth of one or both of the phenotypes, indicating an unsuccessful outcome.

Although the analytic description of the eigenvalues is messy, it is not difficult. We find that one of the eigenvalues is less than one for all nonzero dose/withdrawal times. The other eigenvalue is more interesting. For the parameters shown in Table I, we plot the curve in the (Td, Tw) -axis for which the second eigenvalue is equal to one (see Figure 12). Above this curve the eigenvalue is less than one, while below this curve the eigenvalue is greater than one. This corresponds to successful/unsuccessful treatment respectively. We also show the value of the eigenvalue for fixed dose time and varying withdrawal times in Figure 13. This curve agrees qualitatively with the simulations shown in Section 3.2. In particular, we see that for short withdrawal times, we have successful treatment and that the speed at which the populations decrease to zero has a unique minimum. For long withdrawal times the eigenvalue is greater than one, indicating an unsuccessful treatment. Both the withdrawal time which precludes successful treatment and the optimal withdrawal time are similar to those obtained in Section 3.2.

We also see that for withdrawal time larger than 9.3, there is no successful treatment for. Although the results are shown only for $Td = 0$ to 5 hours, this conclusion is true for much larger (i.e. $Td > 40$ hours). The withdrawal time along with unbounded growth produces too many bacteria for the treatment to be effective.

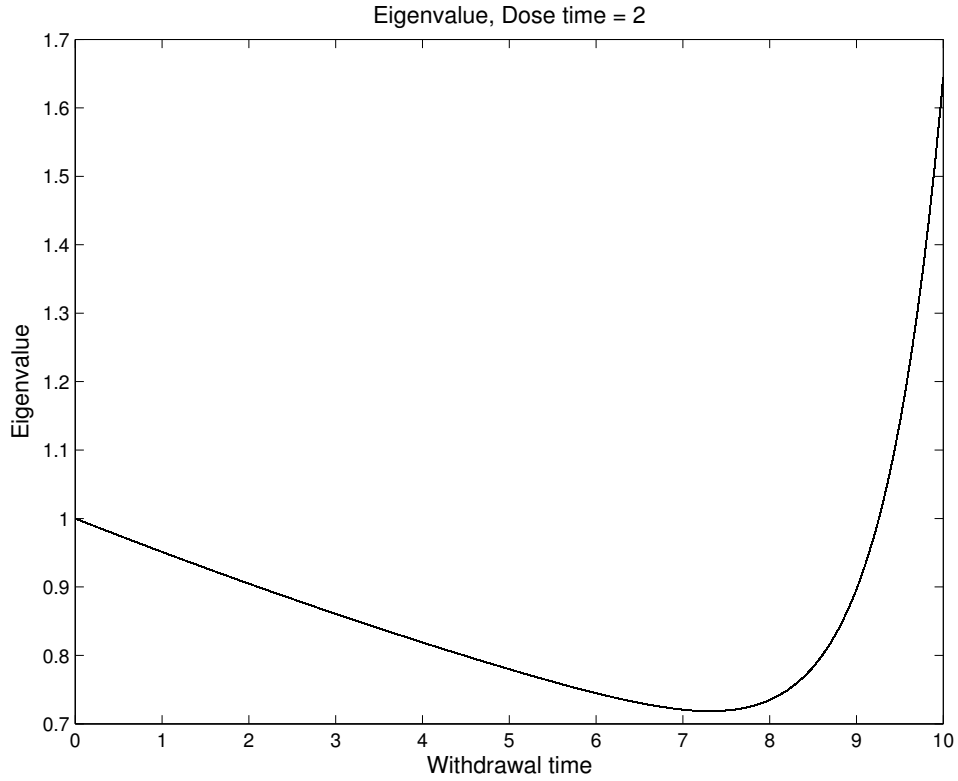


Figure 13: We show the value of the eigenvalue for fixed $Td = 2$ as a function of the withdrawal time. We see that for withdrawal times less than approximately nine hours, the eigenvalue is less than one, indicating a successful treatment. The minimum value occurs at approximately 7.5 hours, which agrees well with results from Section 3.2.

5 Discussion

We have presented a mathematical model of bacterial tolerance based experimentally observed 'persister cells', which are assumed to be a dormant phenotype that is expressed at a rate that depends on the population growth rate and the antibiotic concentration. Parameters of the model have been chosen to yield results comparable to experiments. The model is used to show that alternating dose/withdrawal of the antibiotic can eliminate the bacteria. Moreover, the optimal dose/withdrawal times can be computed. A simplified model is analyzed, indicating dramatic difference in the behavior for varying dose and withdrawal times.

Because we assume that the rate of persister formation is proportional to the growth rate, we find that persister cells are formed throughout the growth-cycle. This is not reflected in experimental results (Dr. Kim Lewis personal communication). Instead, it seems that there is no persister formation until the mid to late exponential phase. This may indicate that the expression of the persister phenotype is regulated by an auto-inductive signal; however, in the absence of any direct physiological evidence, we feel that our results are indicative of persister dynamics.

References

- [1] L. ADAMS AND T. CHARTER, *New geometric immersed interface multigrid solvers*, SIAM Journal on Scientific Computing, 25 (2004), pp. 1516–1533.
- [2] D. ALLISON AND P. GILBERT, *Modification by surface association of antimicrobial susceptibility of bacterial populations*, Journal of Industrial Microbiology, 15 (1995), pp. 311–317.
- [3] M. ASHBY, J. NEALE, AND I. CRITCHLEY, *Effect of antibiotics on non-growing planktonic cells and biofilms of Escherichia coli*, Journal of Antimicrobial Chemotherapy, 33 (1994), pp. 443–452.
- [4] N. BAGGE, M. HENTZER, J. B. ANDERSON, O. CIOFU, M. GIVSKOV, AND N. HOIBY, *Dynamics and spatial distribution of β -lactamase expression in Pseudomonas aeruginosa biofilms*, Antimicrobial Agents and Chemotherapy, 48 (2004), pp. 1168–1174.
- [5] A. BROOUN, J. TOMASHEK, AND K. LEWIS, *A dose-response study of antibiotic resistance in Pseudomonas aeruginosa biofilm*, Antimicrobial Agents and Chemotherapy, 44 (2000), pp. 640–646.
- [6] M. BROWN, D. ALLISON, AND P. GILBERT, *Resistance of bacterial biofilms to antibiotics: a growth-rate related effect?*, J. Antimicrob. Chemother., 22 (1988), pp. 777–783.
- [7] W. G. CHARACKLIS AND K. C. MARSHALL, eds., *Biofilms*, John Wiley and Sons, inc., 1990.
- [8] C.-I. CHEN, M. REINSEL, AND R. MUELLER, *Kinetic investigation of microbial souring in porous media using microbial consortia from oil reservoirs*, Biotechnology and Bioengineering, 44 (1994), pp. 263–269.
- [9] N. COGAN, R. CORTEZ, AND L. FAUCI, *Modeling physiological resistance in bacterial biofilms*, Bulletin of Mathematical Biology, (2005). to appear.
- [10] R. CORTEZ, *The method of regularized stokeslets*, SIAM Journal of Scientific Computing, 23 (2001), pp. 1204–1224.
- [11] R. CORTEZ, L. FAUCI, AND A. MEDOVIKOV, *The method of regularized stokeslets in three dimensions: Analysis, validation, and application to helical swimming*, Physics of Fluids, (2004).
- [12] J. COSTERTON, P. S. STEWART, AND E. P. GREENBERG, *Bacterial biofilms: A common cause of persistent infections*, Science, 284 (1999), pp. 1318–1322.
- [13] D. DAVIES, *Understanding biofilm resistance to antibacterial agents*, Nature Reviews Drug Discovery, 2 (2003), pp. 114–122.

- [14] D. DAVIES, M. PARSEK, J. COSTERTON, J. PEARSON, B. IGLESKI, AND E. GREENBERG, *The involvement of cell-to-cell signals in the development of a bacterial biofilm*, Science, 280 (1998).
- [15] D. DEBEER, R. SRINIVASAN, AND P. S. STEWART, *Direct measurement of chlorine penetration into biofilms during disinfection*, Applied Environmental Microbiology, 60 (1994), pp. 4339–4344.
- [16] M. DESAI, T. BUHLER, P. WELLER, AND M. BROWN, *Increasing resistance of planktonic and biofilm cultures of Burkholderia cepacia to ciprofloxacin and ceftazidime during exponential growth*, Journal of Antimicrobial Chemotherapy, 42 (1998), pp. 153–160.
- [17] M. G. DODDS, K. J. GROBE, AND P. S. STEWART, *Modeling biofilm antimicrobial resistance*, Biotechnology and Bioengineering, 68 (2000), pp. 456–465.
- [18] E. DRENKARD AND F. M. AUSUBEL, *Pseudomonas biofilm formation and antibiotic resistance are linked to phenotypic variation*, Nature, 416 (2002), pp. 740–743.
- [19] J. G. ELKINS, D. J. HASSETT, P. S. STEWART, H. P. SCHWEIZER, AND T. R. MCDERMOTT, *Protective role of catalase in Pseudomonas aeruginosa biofilm resistance to hydrogen peroxide*, Applied and Environmental Microbiology, 65 (1999), pp. 4594–4600.
- [20] P. GILBERT, T. MAIRA-LITRAN, A. J. MCBAIN, A. H. RICKARD, AND F. W. WHYTE, *The physiology and collective recalcitrance of microbial biofilm communities*, Advances in Microbial Physiology, 46 (2002), pp. 202–256.
- [21] B. GIWERCMAN, E. JENSEN, N. HOIBY, A. KHARAZMI, AND J. COSTERTON, *Induction of β -lactamase production in Pseudomonas aeruginosa biofilm*, Antimicrobial Agents and Chemotherapy, 35 (1991), pp. 1008–1010.
- [22] G. H. GOLUB AND C. F. V. LOAN, *Matrix Computations*, Johns Hopkins University Press, 3 ed., 1996.
- [23] K. GROBE, J. ZAHLER, AND P. STEWART, *Role of dose concentration in biocide efficacy against Pseudomonas aeruginosa biofilms*, Journal of Industrial Microbiology and Biotechnology, 29 (2002), pp. 10–15.
- [24] M. HENTZER, H. WU, J. B. ANDERSEN, K. RIEDEL, T. B. RASMUSSEN, N. BAGGE, N. KUMAR, M. A. S. ND ZHIJUN SONG, P. KRISTOFFERSEN, M. MANEFIELD, J. W. COSTERTON, S. MOLIN, L. EBERL, P. STEINBERG, S. KJELLEBERG, N. HOIBY, AND M. GIVSKOV, *Attenuation of Pseudomonas aeruginosa virulence by quorum sensing inhibitors*, The EMBO Journal, 22 (2003), pp. 3803–3815.
- [25] I. KEREN, N. KALDALU, A. SPOERING, Y. WANG, AND K. LEWIS, *Persister cells and tolerance to antimicrobials*, FEMS Microbiology Letters, 230 (2004), pp. 13–18.

- [26] T. R. D. KIEVIT, M. D. PARKINS, R. J. GILLIS, R. SRIKUMAR, H. CERI, K. POOLE, B. H. IGLEWSKI, AND D. G. STOREY, *Multidrug efflux pumps: Expression patterns and contribution to antibiotic resistance in Pseudomonas aeruginosa biofilms*, *Antimicrobial Agents and Chemotherapy*, 45 (2001), pp. 1761–1770.
- [27] I. KLAPPER, C. RUPP, R. CARGO, B. PURVEDORJ, AND P. STOODLEY, *Viscoelastic fluid description of bacterial biofilm material properties*, *Biotechnology and Bioengineering*, 80 (2002), pp. 289–296.
- [28] H. KUMON, K. TOMOCHIKA, T. MATUNAGA, M. OGAWA, AND H. OHMORI, *A sandwich cup method for the penetration assay of antimicrobial agents through Pseudomonas exopolysaccharides*, *Microbiology Immunology*, 38 (1994), pp. 615–619.
- [29] H. M. LAPPIN-SCOTT AND J. W. COSTERTON, eds., *Microbial Biofilms*, Cambridge University Press, Cambridge, 1995, ch. Mechanisms of the Protection of Bacterial Biofilms from Antimicrobial Agents, pp. 118–130.
- [30] R. J. LEVEQUE AND Z. LI, *The immersed interface method for elliptic equations with discontinuous coefficients and singular sources*, *SIAM Journal of Numerical Analysis*, 31 (1994), pp. 1019–1044.
- [31] K. LEWIS, *Riddle of biofilm resistance*, *Antimicrobial Agents and Chemotherapy*, 45 (2001), pp. 999–1007.
- [32] J. M. LIGHTHILL, *An informal introduction to theoretical fluid mechanics*, Oxford University Press, New York, 1986.
- [33] T. MAH, B. PITTS, B. PELLOCK, G. WALKER, P. STEWART, AND G. O’TOOLE, *A genetic basis for Pseudomonas aeruginosa biofilm antibiotic resistance*, *Nature*, 426 (2004), pp. 306–310.
- [34] J. MANEM AND B. RITTMANN, *Removing trace level organic pollutants in a biological filter.*, *Journal of American Water Works*, 84 (1992), pp. 152–157.
- [35] C. PICIOREANU, M. C. VAN LOOSDRECHT, AND J. J. HEIJNAN, *Two-dimensional model of biofilm detachment caused by internal stress from liquid flow*, *Biotechnology and Bioengineering*, 72 (2001), pp. 205–218.
- [36] C. POTERA, *Forging a link between biofilms and disease*, *Science*, 283 (1999), pp. 1837–1839.
- [37] C. POZRIKIDIS, *Numerical computation in science and engineering*, Oxford University Press, New York, 1998.
- [38] B. PRAKASH, B. VEEREGOWDA, AND G. KRISHNAPPA, *Biofilms: A survival strategy of bacteria*, *Current Science India*, 85 (2003), pp. 1299–1307.
- [39] M. E. ROBERTS AND P. S. STEWART, *Modeling antibiotic tolerance in biofilms by accounting for nutrient limitation*, *Antimicrobial Agents and Chemotherapy*, 48 (2004), pp. 48–52.

- [40] —, *Modelling protection from antimicrobial agents in biofilms through the formation of persister cells*, *Microbiology*, 151 (2005), pp. 75–80.
- [41] S. S. SANDERSON AND P. S. STEWART, *Evidence of bacterial adaption to monochloramine in Pseudomonas aeruginosa biofilms and evaluation of biocide action model*, *Biotechnology and Bioengineering*, 56 (1997), pp. 201 – 209.
- [42] A. SPOERING AND K. LEWIS, *Biofilms and planktonic cells of Pseudomonas aeruginosa have similar resistance to killing by antimicrobials.*, *Journal of Bacteriology*, 183 (2001), pp. 6746–6751.
- [43] P. S. STEWART, *Diffusion in biofilms*, *Journal of Bacteriology*, 185 (2003), pp. 1485–1491.
- [44] P. S. STEWART, F. ROE, J. RAYNER, J. G. ELKINS, Z. LEWANDOWSKI, U. A. OCHSNER, AND D. J. HASSETT, *Effect of catalase on hydrogen peroxide penetration into Pseudomonas aeruginosa biofilms*, *Applied and Environmental Microbiology*, 66 (2000), pp. 836–838.
- [45] N. SUFYA, D. ALLISON, AND P. GILBERT, *Clonal variation in maximum specific growth rate and susceptibility towards antimicrobials*, *Journal of Applied Microbiology*, 95 (2003), pp. 1261–1267.
- [46] O. WANNER AND P. REICHERT, *Mathematical modeling of mixed-culture biofilms*, *Biotechnology and Bioengineering*, 49 (1996), pp. 172–184.
- [47] J. WINGENDER, T. R. NEU, AND H.-C. FLEMING, *Microbial Extracellular Polymeric Substances. Characterization, Structure and Function*, Springer Verlag, 1999.
- [48] K. XU, P. STEWART, F. XIA, C.-T. HUANG, AND G. MCFETERS, *Spatial physiological heterogeneity in Pseudomonas aeruginosa biofilm is determined by oxygen availability*, *Applied Environmental Microbiology*, 64 (1998), pp. 4035–4039.
- [49] K. D. XU, G. A. MCFETERS, AND P. STEWART, *Biofilm resistance to antimicrobial agents*, *Microbiology*, 146 (2000).
- [50] X. XU, P. STEWART, AND X. CHEN, *Transport limitation of chlorine disinfection of Pseudomonas aeruginosa entrapped in alginate beads*, *Biotechnology and Bioengineering*, 49 (1996), pp. 93–100.
- [51] J. YU, M. JI, AND P. YUE, *A three-phase fluidized bed reactor in the combined anaerobic/aerobic treatment of wastewater*, *Journal of Chemical Technology and Biotechnology*, 74 (1999), pp. 619–626.
- [52] X. ZHANG AND P. L. BISHOP, *Spatial distribution of extracellular polymeric substances in biofilms*, *Journal of Environmental Engineering*, 127 (2001), pp. 850 – 856.